JGR Biogeosciences

RESEARCH ARTICLE
10.1029/2025JG009261

Sedimentary Environment Controls Carbon Sequestration Potential of Unvegetated Intertidal Estuarine Sediments

Andrew D. La Croix[1]

[1]Sedimentary Environments and Analogues Research Group, Earth and Environmental Sciences, School of Science, University of Waikato, Hamilton, New Zealand

Key Points:

- Five distinct sedimentary facies were identified, each with different capacities for organic carbon burial
- Muddy, low-energy areas (upper tidal flats) consistently store more organic carbon than sandy, higher-energy zones (lower tidal flats and channels)
- Changes in sediment supply and estuarine processes over time have influenced long-term carbon storage

Supporting Information:

Supporting Information may be found in the online version of this article.

Correspondence to:

A. D. La Croix,
alacroix@waikato.ac.nz

Citation:

La Croix, A. D. (2025). Sedimentary environment controls carbon sequestration potential of unvegetated intertidal estuarine sediments. *Journal of Geophysical Research: Biogeosciences*, *130*, e2025JG009261. https://doi.org/10.1029/2025JG009261

Received 10 JUL 2025
Accepted 21 NOV 2025

Abstract Unvegetated intertidal sediments are increasingly recognized as contributors to coastal carbon storage, yet their organic carbon burial potential remains poorly constrained. This study examines spatial and temporal patterns of carbon accumulation in unvegetated intertidal flats of Ōhiwa Harbor, New Zealand, using surface sediments and three radiocarbon-dated cores spanning up to ~7,700 yrs. Within the harbor, five distinct sedimentary facies were identified, each displaying unique sediment characteristics and patterns of organic carbon burial. Mud-rich, low-energy facies, including rippled and bioturbated muds, consistently showed higher organic carbon density and burial rates compared to sandy, more dynamic facies. Estimated carbon stocks in the upper meter of sediment range from 44 to 120 t C ha^{-1}, comparable to or exceeding those of many vegetated coastal habitats. Temporal changes in facies distribution driven by estuarine processes and variations in sediment supply led to significant long-term fluctuations in organic carbon burial. These results demonstrate that organic carbon storage in unvegetated intertidal flats is highly heterogeneous and controlled by the persistence of fine-grained depositional environments. A facies-based framework offers a process-driven approach to assessing and managing blue-carbon potential in estuarine systems increasingly altered by climate and land-use change.

Plain Language Summary Unvegetated intertidal areas like mudflats play an important role in storing carbon, but we still don't fully understand how much organic matter they can bury or what controls this process. This study examined how organic matter builds up and is buried in different parts of Ōhiwa Harbor, New Zealand, using surface sediments and three dated sediment cores that record up to about 7,700 yrs of history. Five distinct sediment types were identified, each with unique characteristics and different capacities for storing organic matter. Muddy, low-energy areas consistently contained and buried more organic matter than sandy, more dynamic environments. Over time, changes in estuarine processes and sediment supply altered where these sediment types occurred, leading to fluctuations in organic matter burial. These findings show that carbon storage in unvegetated sediments is highly variable and depends on the persistence of fine-grained, stable environments. Using sediment types as a framework for understanding and managing blue carbon can help protect and enhance carbon storage in coastal systems increasingly affected by climate and land-use change.

1. Introduction

Estuarine sediments are important long-term sinks for organic carbon, mediating the exchange between terrestrial and marine systems and contributing significantly to coastal carbon budgets (Bauer et al., 2013; Bianchi et al., 2018). While vegetated habitats such as salt marshes and mangroves have been extensively studied and are increasingly mapped with fine ecological resolution (e.g., Alongi, 2020; Bulmer et al., 2020; Mcleod et al., 2011; Puppin et al., 2024), unvegetated intertidal flats, despite their widespread distribution and dynamic depositional character, remain underrepresented in carbon storage assessments (e.g., Chen et al., 2020; Lee et al., 2021; Zhou et al., 2024). These bare sediment environments are often treated as homogeneous, with organic matter (OM) and organic carbon (OC) burial estimated using bulk properties such as grain size, where higher OM/OC content is generally associated finer-grained sediment (Mayer et al., 1985). This oversimplification masks critical variability in OM/OC dynamics within estuaries.

Sediment grain size, particularly mud content (particles <62.5 μm), is widely recognized as a key factor controlling OM/OC preservation due to the enhanced surface area and reduced permeability of fine-grained sediments (Burdige, 2007; Hedges & Keil, 1995; Serrano et al., 2016). This increased surface area facilitates the adsorption of OM onto mineral surfaces and the low permeability of fine-grained deposits limits oxygen

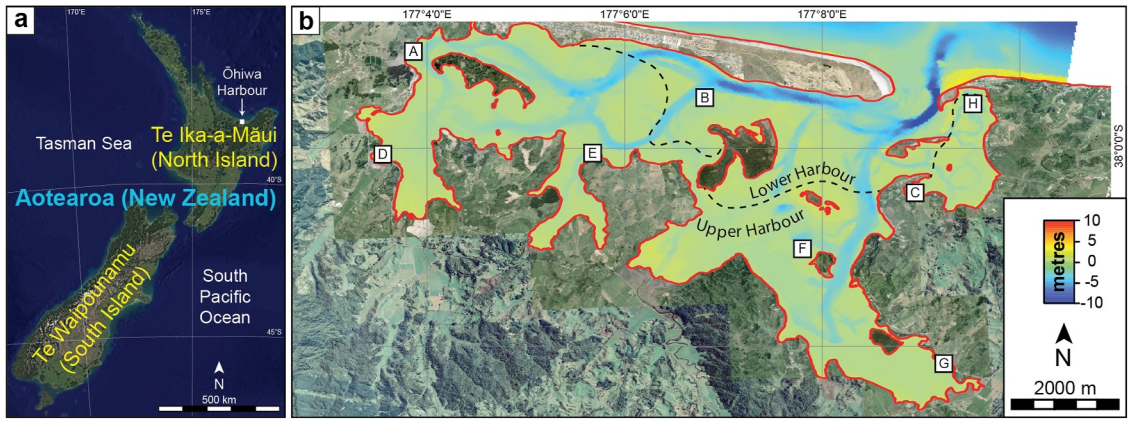

Figure 1. (a) Location of Ōhiwa Harbor in Aotearoa New Zealand. (b) Location of the eight sediment cores analyzed in this study.

diffusion, contributing to the stabilization and long-term burial of organic carbon (Hedges & Keil, 1995; Mayer, 1994). However, this simplification overlooks the complexity of sedimentary environments such as estuaries, where the physical and chemical composition and structure of sediments (i.e., sedimentary facies) can vary markedly over short spatial scales in response to changes in hydrodynamics, deposition rates, and sediment supply (Dalrymple et al., 1992). These variations not only influence OM concentration, but also OM quality, source, and preservation potential, which are important factors affecting long-term carbon sequestration yet are rarely resolved at the facies level.

In this paper it is shown that sedimentary (sub) environments in unvegetated intertidal portions of estuaries have distinct bulk organic matter characteristics. Using sediment cores collected from multiple locations around Ōhiwa Harbor, Aotearoa New Zealand, the spatial-temporal variation in OM content and burial is quantified, revealing consistent differences tied to depositional environment. The findings highlight the need to move beyond bulk estimates and mud-based classifications of OM/OC, and instead incorporate sedimentological context into coastal carbon models to improve predictions of carbon storage in intertidal estuarine systems.

2. Study Area

Ōhiwa Harbor is a shallow estuarine lagoon on the eastern North Island of Aotearoa New Zealand (Figure 1). It is sheltered from the Bay of Plenty by the Ōhope and Ōhiwa sand spits, with a 600 m-wide tidal inlet at high tide. The harbor covers an area of 24 km^2, has a 48 km perimeter, with up to 70% of its area exposed at low tide (Gibb, 1977; Richmond et al., 1984). Broad tidal flats with slopes of less than 3° rim the harbor, generally having topographic relief of less than 1 m (Richmond et al., 1984).

The upper flats (~40% of intertidal area) are vegetated in places with saltmarsh (*Salicornia*, *Juncus*, *Leptocarpus*) and mangroves (*Avicennia resinifera*), while lower flats (~60% of intertidal area) are mostly unvegetated and dissected by tidal creeks (Richmond et al., 1984). Ōhiwa Harbor is a key shellfish harvesting area, and its intertidal flats host dense benthic bivalve assemblages that contribute significantly to biogenic reworking and the accumulation of shell-rich substrates.

Mean depth in Ōhiwa Harbor is 2 m, with a maximum depth of 14 m, and a volume at high tide of 49.4×10^6 m^3 (Freestone, 1976; Richmond et al., 1984). Tides are semidiurnal with a neap-spring range of 1.6–2.5 m. Water flow in the harbor is overwhelmingly dominated by tidal currents, with velocities up to 125 cm s^{-1} through the mouth of the inlet (Freestone, 1976; Richmond et al., 1984). Freshwater discharge into the harbor is very small, approximately 1.2 m^3 s^{-1} (Freestone, 1976), with a similarly small land-derived sediment supply. Most sediment is carried into the mouth of Ōhiwa Harbor by eastward flowing longshore currents from the Whakatāne River (Healy, 1978). Tidal flushing of the lagoon is rapid with a water residence time of only 1–2 tidal cycles (Richmond et al., 1984). Wind-induced waves along the margins of the harbor can reach heights up to 0.5 m, with predominantly northwesterly, northerly, and southerly directions of propogation (Richmond et al., 1984). Recent hydrodynamic modeling shows that tidal flows are spatially variable, with strong current velocities and sand

transport near the entrance, while fine sediment and organic material accumulate in the upper, low-energy flats (Bryan et al., 2023).

The harbor is situated on the eastern end of the Whakatāne Graben, which is subsiding at a rate of 1–2 mm yr^{-1} (Beanland & Berryman, 1992), and lies adjacent to the uplifting Raukumara Ranges, between the Ōhope and Waikaremoana faults (Beanland & Berryman, 1992; Hayward et al., 2004). The hills surrounding Ōhiwa Harbor comprise mid-Pleistocene sedimentary strata of the Ōhope Formation, which rests unconformably atop Mesozoic greywacke (Healy, 1967). These pass upwards into late-Pleistocene sedimentary strata and tephras of the Waiotahi Gravels and Ōhiwa Harbor Subgroup, respectively (Manning, 1996). The inner harbor of Ōhiwa overlies Pleistocene sedimentary rocks and tuffs of the Huka Group, but islands within the harbor may also consist of consolidated modern sediments (i.e., Tern and Motuotu islands) (Richmond et al., 1984).

The mineralogy of sediment diverges somewhat between the upper harbor and lower harbor. In the upper harbor (distant to the main tidal channel and harbor mouth; sensu Richmond et al., 1984) sediments are dominated by volcanic glass, pumice fragments, and feldspar, with subordinate amounts of quartz and biogenic calcite. These sediments often include shell fragments that are partially broken or reworked by benthic fauna and wave action, particularly in the unvegetated lower tidal flats. By contrast the lower harbor (proximal to the main tidal channels and harbor mouth; sensu Richmond et al., 1984) is enriched in quartz and feldspar, with relatively less volcanic material. Bioturbation in the lower tidal flats is generally higher, producing abundant burrows and surface reworking, which can mix finer organic-rich sediments with coarser shell material and modify primary sedimentary structures (Richmond et al., 1984).

Ōhiwa Harbor formed as sea levels rose from a position 134 m lower than present at 21,000 yrs ago, stabilizing about 7,000 yrs ago (Lambeck et al., 2014). Barrier formation followed the mid-Holocene stillstand (7,410 –5,175 yrs ago), with the harbor's current configuration emerging about 575 yrs ago (Julian, 2006; Murdoch, 2005).

3. Methods

To assess the OM and OC characteristic of unvegetated intertidal sediments in Ōhiwa Harbor, cores ($n = 8$) and surface sediments ($n = 73$) were collected from eight stations: Sites A–G and Cores A–H, respectively (Figure 1b; Table S1 in Supporting Information S1). Sites were named in order of data collection with no surface sediment samples collected around Core H. Cores ranged in thickness from 2.09 to 3.38 m thick. Surface sediments were collected in a grid pattern around the cores, with grid spacing ranging from 50 to 100 m, sampling the upper 0–2 cm of the sediment surface.

After sediment cores were extracted, they were sealed water-tight and transported back to the lab, where they were split in half, x-rayed, logged, and sub-sampled. X-radiographs were collected using a Cubex 50 portable veterinary x-ray source operating at 90 kV and 1.30 mAs. X-rays were detected on a Canon MXD DR9000 flat panel detector. Cores were logged for their grain size and lithology, bioturbation intensity and ethology, physical sedimentary structures, and shells or accessories. Bioturbation intensity was assessed using the semi-quantitative "bioturbation index" of Taylor and Goldring (1993). Sediment was subsampled every 2 cm down core for the first 10 cm (i.e., 0–1 cm to 10–11 cm) and then every 5 cm to their base. Although sampling resolution was increased near the surface to capture potential changes in OM content, down-core trends in OM degradation were not explicitly assessed. Extensive bioturbation throughout the cores indicated thorough sediment mixing, which likely homogenized vertical OM patterns. Therefore, OM degradation with depth was not considered in this study.

Sediment sub-samples from cores, as well as surface sediments, were immediately placed in whirl pack bags to seal in moisture and stored in the dark at 6°C. One set of sediment samples was dried at 60°C for 24 hr, treated with 30% H_2O_2 to remove organics, 10% HCl to remove carbonates, and a 5% Na-hexametaphosphate solution to deflocculate clays. These treated samples were seived through a 2 mm mesh and then run through a Malvern Mastersizer to determine the grain size distribution. Statistical treatment of grain size data used GRADISTAT (Blott & Pye, 2001). A second set of sediment samples was used to measure dry bulk density by determining their volume, oven-drying them at 105°C for 24 hr, and then reweighing the dried samples. These sediments were then heated to 430°C for 4 hr, and then weighed again in a modified version of the loss-on-ignition (LOI) method of Wood (2015). The final difference in mass was considered to be a proxy for OM content.

A third subset of sediments ($n = 42$) were dried at 60°C for 48 hr and then finely ground using a clean mortar and pestle. Approximately 3 g of each sample was acidified with 10% HCl to remove inorganic carbon, followed by multiple rinses with ultrapure water. The acidified sediment was dried overnight at 60°C and reground prior to analysis. Total organic carbon (OC_m) content was measured using a Flash 2,000 elemental analyzer (Thermo Fisher Scientific, Bremen, Germany), which combusts the organic fraction to CO_2 for quantitative carbon measurement. Analytical precision was typically better than ±0.2% based on replicate sample analyses. For clarity, OM refers to organic matter content measured by loss-on-ignition (LOI), OC_m represents organic carbon measured directly using the elemental analyzer, and OC_e denotes organic carbon estimated from an LOI–OC_m regression relationship.

Finally, 24 cockle (*Austrovenus stutchburyi*) shells were selected from 4 cores for accelerator mass spectrometer radiocarbon (AMS ^{14}C) dating. Shells were cleaned, washed in an ultrasonic bath, tested for recrystallization of aragonite, and then acid washed in 0.1 N hydrochloric acid. Radiocarbon preparation and analysis was undertaken at the University of Waikato Radiocarbon lab. All AMS ^{14}C ages were corrected for isotopic fractionation using $\delta^{13}C$ values. Conventional ages were converted into calendar yrs BP using Oxcal v4.4.4 (Bronk Ramsey, 1995) with the Marine20 calibration curve (Heaton et al., 2020) and a marine reservoir offset of -154 ± 38 (Petchey 2025 pers. comm). rBacon was used for Bayesian age-depth modeling of three of the four sediment cores based on radiocarbon dates (Blaauw & Christen, 2011).

Statistical analyses were carried out in Python. The data were generally not normally distributed, and therefore, non-parametric tests were used throughout. The Kendall τ test was applied to explore monotonic relationships between key variables, while the Kruskal–Wallis H test was used to test for differences in OM content among sedimentary facies. Where the Kruskal–Wallis results indicated significant differences, Dunn's post hoc test was then used to identify which facies pairs were distinct. All available data were retained in these analyses, and no attempt was made to remove potential outliers.

4. Results

4.1. Surface Sediment Distribution

The proportion of mud in surface sediments varies considerably across locations. Site A has a mean mud content of 45% (range: 20.8%–82.8%; Figure 2). Mud content at Site B is 18% on average (range: 1.6%–25.0%). Site C shows a mean of 32% mud (range: 7.6%–53.1%). The mean mud content at Site D is 58% (range: 11.9%–90.0%). Site E displays a mean mud content of 20% (range: 11.9%–30.6%). Site F has a mean of 21% (range: 3.8%–39.0%). And finally, Site G has the highest mean mud content at 66% (range: 47.1%–89.9%). Organic matter also varies across locations with Site A displaying a mean of 2.36% (range: 1.50%–3.56%; Figure 3). Site B has a mean of 2.00% (range: 1.31%–2.43%). The mean OM at Site C is 1.91% (range: 1.28%–2.57%). Site D has the highest OM, with a mean of 2.99% (range: 1.74%–6.24%). Site E has a mean OM of 1.96% (range: 1.48%–2.34%). Site F shows a mean of 1.89 t% (range: 1.19%–2.51%), and Site G has a mean OM of 2.76% (range: 2.41%–3.99%).

4.2. Sedimentary Facies and Facies Associations

Analysis of sediment cores indicates that the uppermost ~3 m of intertidal sediments in Ōhiwa Harbor comprise five sedimentary facies (Figure 4; Table 1). Facies 1 is muddy shell bed, that is interpreted as the dense life assemblage, forming shell banks on tidal flats (Figures 4a and 5; Table 1; Richmond et al., 1984). An alternative interpretation for the muddy shell beds is that they represent channel lag deposits, but this interpretation is rejected because the facies does not occur below other channel deposits. Facies 2 comprises rippled to cross bedded sand, interpreted to be the product of migrating subaqueous dunes and ripples in tidal creeks and channels (Figures 4b and 5; Table 1; Richmond et al., 1984). Facies 3 consists of bioturbated sand, gravelly silty sand, or silty sand, produced by thorough mixing of sandy substrates on the lower tidal flat (i.e., Facies 2; Figures 4c and 5; Table 1; Richmond et al., 1984). Facies 4 is composed of rippled to planar-laminated silts, deposited from low to moderate-concentration cohesive flows near the transition between turbulent to quasi-laminar regimes on the upper tidal flat (Baas & Best, 2008; La Croix & Gingras, 2021; La Croix et al., 2025; MacKay & Dalrymple, 2011) (Figures 4d and 5; Table 1). Finally, Facies 5 is bioturbated sandy silt and silt, resulting from the thorough biogenic mixing of silty substrates on the upper tidal flat (i.e., Facies 4; Figures 4e and 5; Table 1; Richmond et al., 1984).

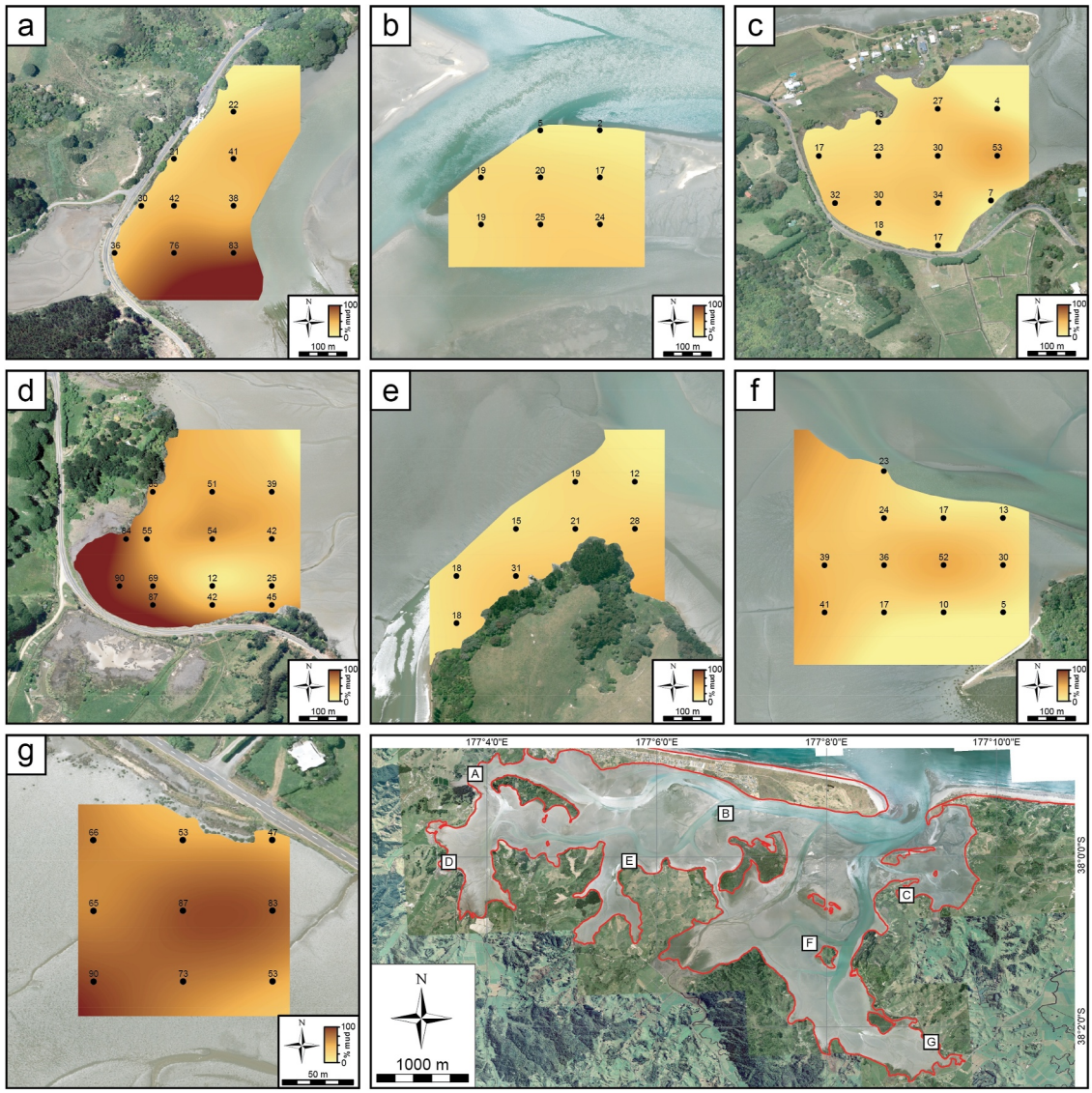

Figure 2. Maps showing proportion of mud (<62.5 μm) in surface sediments in seven of the eight study locations: (a) Site A, (b) Site B, (c), Site C, (d) Site D, (e) Site E, (f) Site F, (g) Site G. Note no surface samples were collected from Site H. Numbers next to black dots represent mud content.

Sedimentary facies in Ōhiwa Harbor group naturally into 2 facies associations (Figure 5). Tidal flat deposits (Facies Association 1) are generally mud-rich, comprising laminated or rippled muds, bioturbated sandy muds, and localized shell beds, and form under relatively low-energy conditions where fine sediments accumulate and biological reworking is pronounced. Tidal channel deposits (Facies Association 2) are dominated by sand-rich units, particularly rippled and cross-bedded sands, reflecting active transport under higher-energy tidal currents. These associations illustrate the contrast between energetic, channelized flow and quieter intertidal flat environments. Most cores were collected near the margins of the harbor, and therefore, the observed sedimentary succession is dominated by Facies Association 1. However, in cores collected from more active areas of the harbor (e.g., Cores B, C, and F), tidal channel deposits were likely more common but may now be largely obscured or homogenized by intense bioturbation, making them difficult to distinguish in the present record.

4.3. Organic Matter Content

Organic matter content varies systematically in different facies (Figures 5 and 6a). Facies F1 averages 2.30% OM (range: 1.29%–4.94%), with the minimum value in Core H at a depth of 236 cm and the maximum in Core A at 101 cm. Facies F2 has the lowest average OM (1.73%; range: 0.92%–2.48%), with a minimum in Core B at

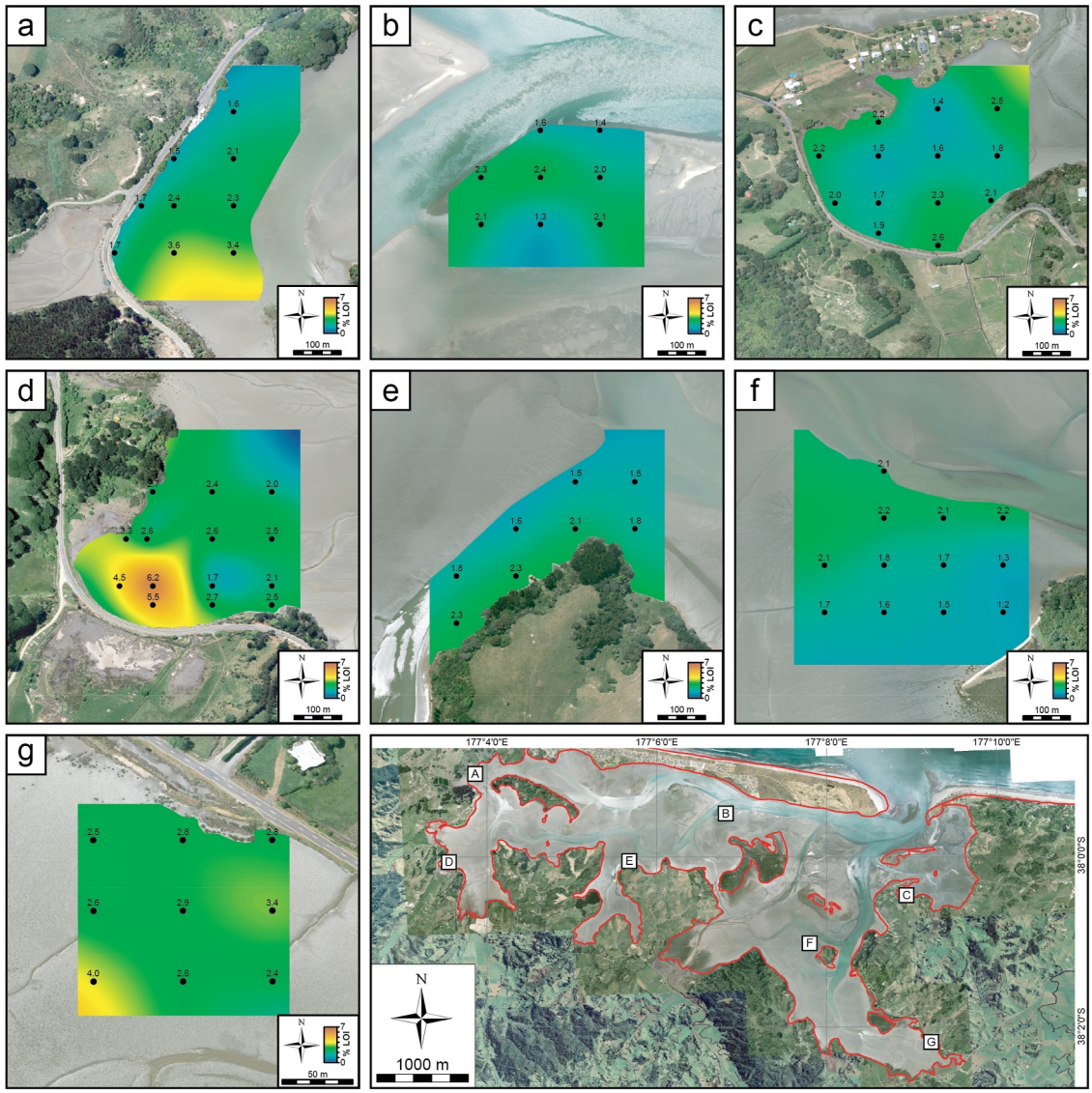

Figure 3. Maps showing OM content (weight % LOI) in surface sediments for seven of the eight study locations: (a) Site A, (b) Site B, (c), Site C, (d) Site D, (e) Site E, (f) Site F, (g) Site G. No surface samples were collected from Site H. Numbers next to black dots represent LOI.

226 cm and maximum in Core F at 171 cm depth. Facies F3 averages 2.43% OM (range: 1.08%–6.24%), which is minimum in Core D at 61 cm depth and maximum at the surface in the vicinity of Core D. Facies F4 is the most organic-rich (mean: 4.99%; range: 2.62%–9.14%), with a minimum in Core B at 166 cm and a maximum in Core G at 126 cm depth. Facies F5 averages 3.04% OM (range: 1.58%–5.10%), which is minimum in Core H at 146 cm depth and maximum in Core D at 296 cm depth.

When all data are considered collectively, without separating by facies classes (Figure 7a), OM content shows a statistically significant inverse relationship with mean grain size, as indicated by a Kendall's tau coefficient of $\tau = -0.4531$ ($p < 0.00001$). This suggests that OM content tends to decrease as grain size increases. Additionally, OM content is positively associated with the proportion of mud, in a statistically significant but non-linear manner (Figure 7b). The corresponding Kendall's tau coefficient is $\tau = 0.4256$ ($p < 0.00001$), indicating that higher mud content is generally linked to increased OM accumulation.

A Kruskal–Wallis test indicates statistically significant differences in OM content across the facies (Table S2 in Supporting Information S1; H = 132.4, $p = 1.20 \times 10^{-27}$). Subsequent post-hoc pairwise comparisons using Dunn's test reveal that Facies F4 and F5 differ significantly from other facies (Figure 8a), while no significant

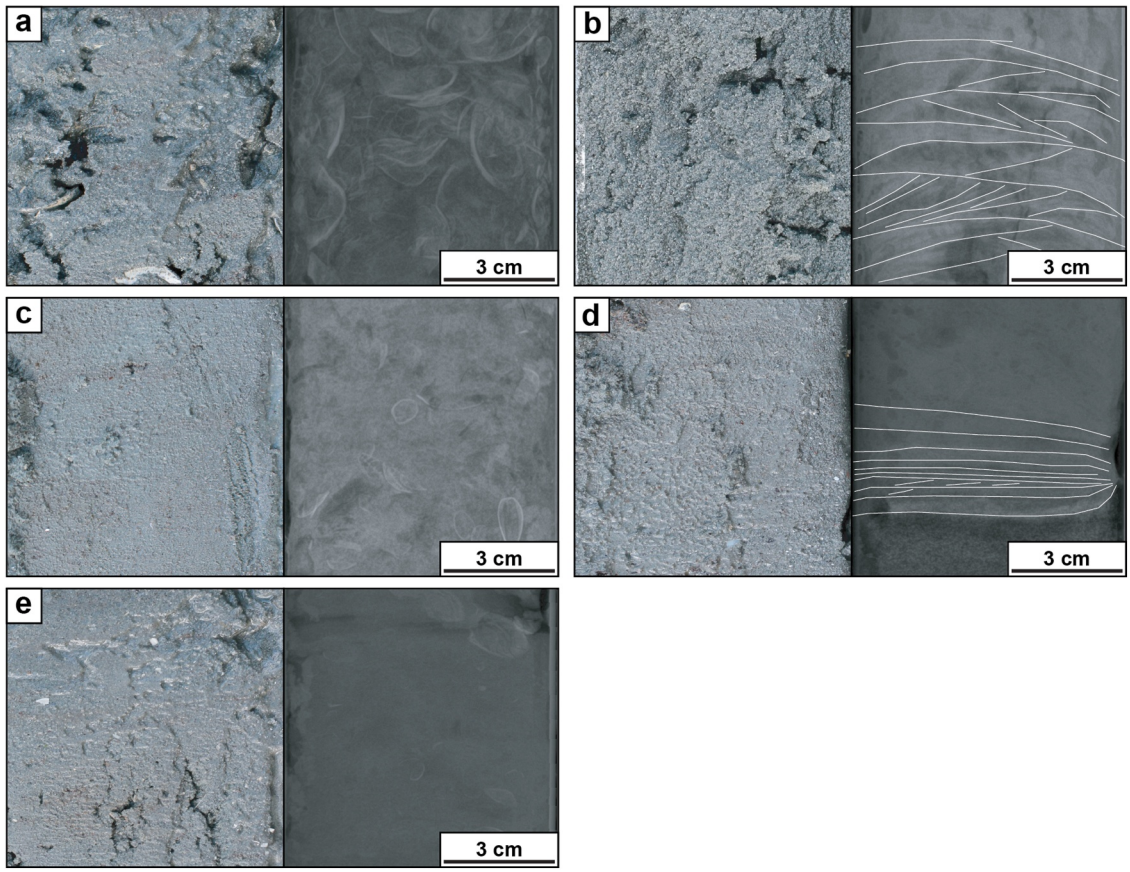

Figure 4. Core photographs and x-radiographs of the five sedimentary facies encountered in unvegetated intertidal portions of Ōhiwa Harbor. (a) Bivalve-gastropod shell bed with mud matrix (Facies 1) from Core A, 16–23 cm depth. (b) Rippled sand (Facies 2) from Core F, 144–151 cm depth. (c) Bioturbated muddy sand with scattered shell fragments (Facies 3) from Core C, 114–120 cm depth. (d) Laminated to rippled mud (Facies 4) from Core A, 146–153 cm depth. (e) Bioturbated sandy mud with shell fragments (Facies 5) from Core A, 54–61 cm depth.

differences are observed among Facies F1, F2, and F3. Collectively, these results demonstrate that both sediment texture and facies type exert strong control on OM variability across the study area.

4.4. Dry Bulk Density

The observed trends in OM content correspond closely with variations in dry bulk density (Figure 6b). Facies F1 has an average dry bulk density of 1.31 g cm^{-3} (range: 1.14–1.41 g cm^{-3}). The minimum density occurs in Core A at 101 cm depth, and the maximum density occurs at the surface in the vicinity of Core A. Facies F2 shows a higher average dry bulk density of 1.35 g cm^{-3} (range: 1.27–1.45 g cm^{-3}), with the minimum in Core F at 116 cm and the maximum in Core B at 226 cm depth. Facies F3 records an average density of 1.32 g cm^{-3}, but with the broadest range (1.09–2.60 g cm^{-3}); its minimum occurs at the surface near Core D and its maximum at the surface near Core C. Facies F4 displays the lowest average dry bulk density among facies at 1.14 g cm^{-3} (range: 0.89–1.29 g cm^{-3}), with the minimum in Core G at 126 cm and the maximum in Core B at 166 cm depth. Facies F5 shows moderate dry bulk density values, averaging 1.27 g cm^{-3} (range: 1.09–1.40 g cm^{-3}), with the minimum recorded in Core E at 106 cm depth and the maximum in Core C at 131 cm depth. Across all samples, dry bulk density shows a strong inverse relationship with OM, following the empirical relation (Figure 7c):

$$\text{Dry Bulk Density} = \frac{1}{\left[\frac{\text{OM}}{0.203} + \frac{(1-\text{OM})}{1.521}\right]} \quad (1)$$

Journal of Geophysical Research: Biogeosciences 10.1029/2025JG009261

Table 1
Sedimentologic Characteristics of the Five Recurring Sedimentary Facies, Along With Their Interpreted Mode of Formation and Environmental Interpretation

Facies	Thickness	Grain size	Physical structures	Bioturbation intensity	Accessories	Process interpretation	Environmental interpretation
Facies 1: Muddy Shell Bed	2–35 cm	More than 30% shells that are >2 mm. Predominantly silt matrix	Rare faint bedding	BI 5–6	Predominantly comprises bivalve shells, with subordinate gastropods	Dense life assemblage on tidal flats	Shell bank
Facies 2: Rippled to Cross Bedded Sand	6–130 cm	Fine sand to medium sand	Low-angle tabular cross beds, current ripples, wave ripples	BI 0–3	None	Shifting sandy subaqueous dunes and ripples	Tidal channels
Facies 3: Bioturbated Sand, Gravelly Muddy Sand, and Muddy Sand	16–44 cm	Very fine sand to coarse sand	None preserved	BI 5–6	Scattered bivalve and gastropod shells, shell layers less than 50% shell material, comminated plant debris	Long-term reworking of sandy substrates	Lower Tidal Flat
Facies 4: Laminated to Rippled Mud	14–35 cm	Fine silt to coarse silt	Current ripples, wavy-undulatory laminae, planar parallel lamination	BI 0–2	None	High-concentration cohesive flows transitioning between weakly turbulent (rippled) and quasi-laminar plug flow (laminated) conditions	Upper Tidal Flat
Facies 5: Bioturbated Sandy Mud and Mud	7–84 cm	Fine silt to coarse silt	Rare normal graded laminae	BI 4–6	Scattered bivalve and gastropod shells, shell layers less than 50% shell material, comminated plant debris	Biological reworking of muddy substrates	Upper Tidal Flat

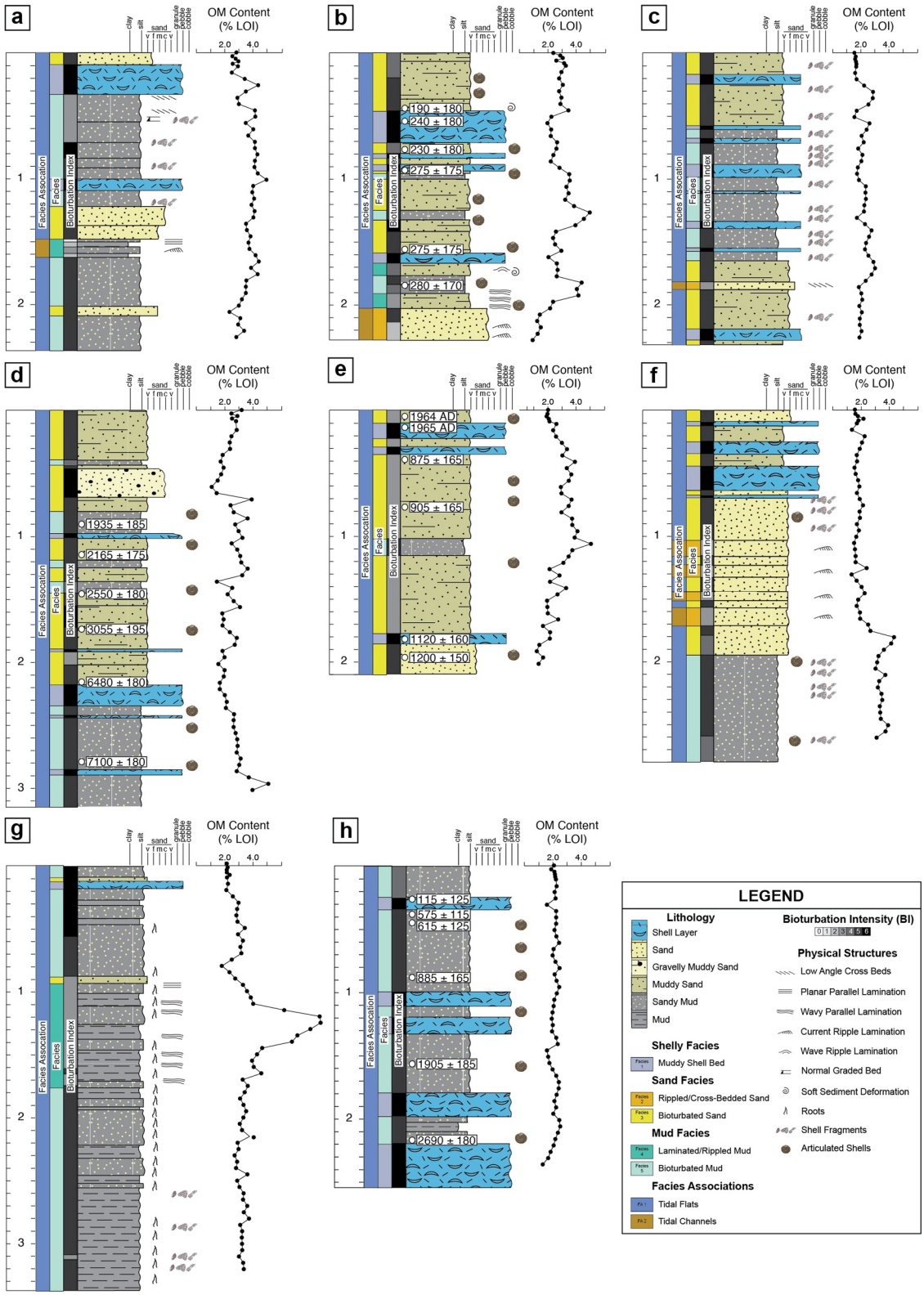

Figure 5. Lithologs of cores collected from Ōhiwa Harbor's unvegetated intertidal flats displaying the stratigraphic distribution of lithology, facies and facies associations, AMS radiocarbon ages, and OM content. (a) Core A, (b) Core B, (c) Core C, (d) Core D, (e) Core E, (f) Core F, (g) Core G, and (h) Core H.

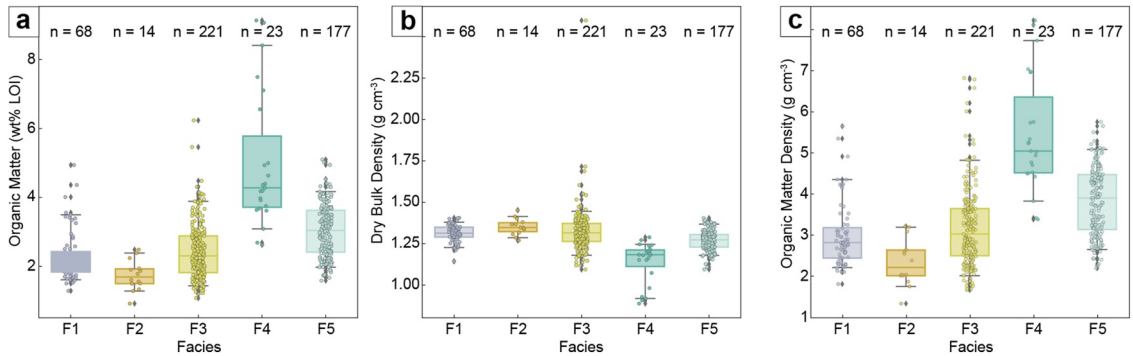

Figure 6. Box and whisker plots showing variation in: (a) OM content (wt % LOI), (b) dry bulk density (g cm^{-3}), and (c) organic matter density (g cm^{-3}) by facies. Boxes mark the median, 25th percentile, and 75th percentile, respectively. Whiskers extend to the most extreme values not considered outliers.

This relation reflects the contrasting densities of organic and mineral components, where increasing OM content leads to lower bulk density.

Kruskal–Wallis statistical testing confirms significant differences in dry bulk density between facies (Table S2 in Supporting Information S1; H = 93.4, $p = 2.45 \times 10^{-19}$). Dunn's test identifies significant contrasts between Facies F4 and other facies, and between Facies F5 and most others, while Facies F1, F2, and F3 are generally not distinct (Figure 8c).

4.5. Organic Matter Density

Mean OM density varies across facies (Figure 6c). In Facies F1, OM density has a mean of 0.030 g cm^{-3} (range: 0.018–0.057 g cm^{-3}). The minimum value occurs in Core H at 236 cm, and the maximum in Core A at 101 cm depth. Facies F2 displays a mean OM density of 0.023 g cm^{-3} (range: 0.013–0.032 g cm^{-3}), with a minimum in Core B at 226 cm and maximum in Core F at 126 cm. Facies F3 shows OM density with a mean of 0.032 g cm^{-3} (range: 0.017–0.068 g cm^{-3}). The minimum occurs in Core D at 61 cm depth, while the maximum is at the surface near Core D. Facies F4 has a mean OM density of 0.055 g cm^{-3} (range: 0.034–0.082 g cm^{-3}), with a minimum values in Core B at 166 cm and maximum value in Core G at 121 cm depth. Finally, Facies F5 displays a mean OM density of 0.038 g cm^{-3} (range: 0.022–0.058 g cm^{-3}). The minimum occurs in Core H at 146 cm, and the maximum in Core B at 126 cm.

OM density also varies significantly by facies according to the Kruskal–Wallis test (Table S2 in Supporting Information S1; H = 131.1, $p = 2.29 \times 10^{-27}$). Dunn's test shows that F4 and F5 are again distinct from most other facies, underscoring the influence of depositional environment on OM preservation (Figure 8d).

4.6. Organic Carbon

Lab measured organic carbon (OC_m) varies between sedimentary facies. Facies F1 has a mean OC_m of 0.72% (range: 0.30%–1.37%), with the lowest value in surface sediments at Site A and the highest in Core A at 31 cm depth. Facies F2 is represented by a single sample, which records 0.17% OC_m (Core F, 146 cm depth). Facies F3

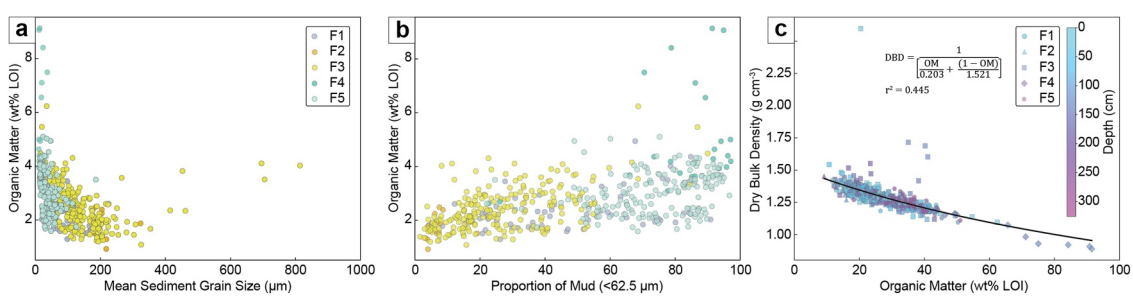

Figure 7. (a) OM content as a function of mean sediment grain size, (b) OM content as a function of proportion of mud, and (c) dry bulk density as a function of OM content.

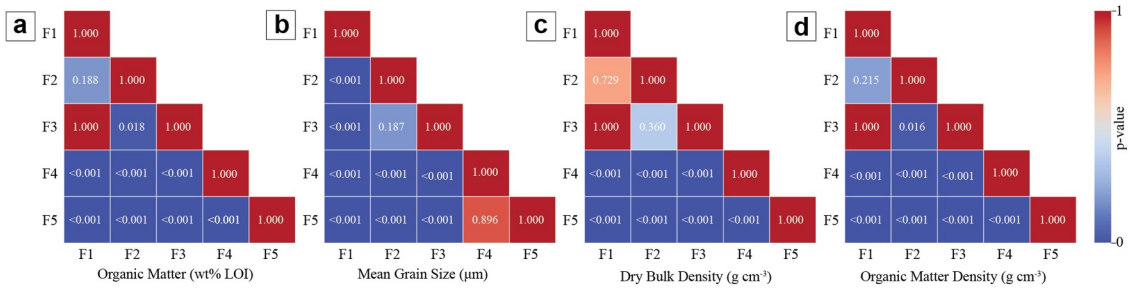

Figure 8. Pairwise statistical comparisons of facies using Dunn's test for four variables: (a) organic matter content (wt % LOI), (b) mean grain size (μm), (c) dry bulk density (g cm^{-3}), and (d) organic matter density (g cm^{-3}). Each cell shows the *p*-value for the difference between facies pairs (Facies F1–F5). Values <0.05 indicate statistically significant differences. Most significant contrasts occur between Facies F4 or F5 and other facies, whereas Facies F1, F2, and F3 show less differentiation.

shows a mean OC_m of 0.49% (range: 0.17%–1.66%), with the minimum in surface sediments at Site C and the maximum in Core B at 9 cm depth. Facies F4 is also represented by a single measurement, showing 2.64% OC_m in Core G at 141 cm depth. Finally, Facies F5 has a mean OC_m of 0.67% (range: 0.33%–1.13%), with the lowest value in surface sediments at Site G and the highest in Core B at 186 cm depth.

For the remaining core and surface sediments, OC was estimated from OM using the linear regression (Figure 9a):

$$OC_e = 34.88\text{LOI} + 0.30 \quad (2)$$

OC_e shows clear variation across different facies (Figure 9b). Facies F1 has an average OC_e of 0.51% (range: 0.15%–1.43%), with the lowest value in Core H at 236 cm depth and the highest in Core A at 101 cm depth. Facies F2 has the lowest mean OC_e at 0.31% (range: 0.02%–0.57%), reaching its minimum in Core B at 226 cm depth and its maximum in Core F at 171 cm depth. Facies F3 averages 0.55% OC_e (range: 0.08%–1.88%), with the minimum found in Core D at 61 cm depth and the maximum at the surface at Site D. Facies F4 is the richest in OC_e, averaging 1.44% (range: 0.62%–2.89%), with the minimum in Core B at 166 cm depth and the maximum in Core G at 126 cm depth. Facies F5 averages 0.76% OC_e (range: 0.26%–1.48%), with the lowest value in Core H at 146 cm depth and the highest in Core D at 296 cm depth.

4.7. Organic Carbon Stocks

Organic carbon stocks in the upper 100 cm of the cores were estimated using facies-specific OC determinations (Figure 10). Stocks ranged from 44 to 120 t C ha^{-1}, with Core A containing the highest stocks (~120 t C ha^{-1}) and Core F the lowest (~44 t C ha^{-1}). The other cores contributed as follows: Core B, 84 t C ha^{-1}; Core C, 56 t C ha^{-1};

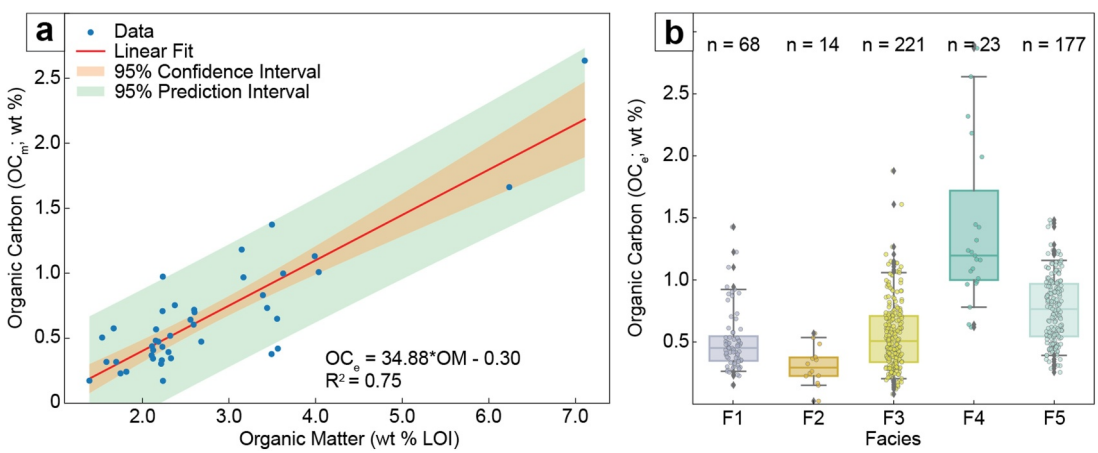

Figure 9. (a) Cross plot of measured organic carbon (OC_m) and organic matter (wt % LOI). The best fit linear regression is displayed, along with the 95% confidence interval and 95% prediction interval. (b) Box and whisker plot showing variation in OC_e (wt %) by facies. Boxes mark the median, 25th percentile, and 75th percentile, respectively. Whiskers extend to the most extreme values not considered outliers.

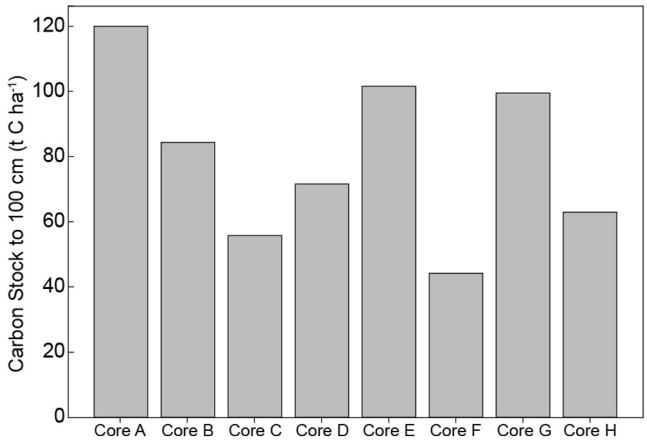

Figure 10. Estimated organic carbon stocks in the upper 100 cm of sediment for cores in Ōhiwa Harbor.

Core D, 72 t C ha^{-1}; Core E, 102 t C ha^{-1}; Core G, 99 t C ha^{-1}; and Core H, 63 t C ha^{-1}. These values offer an integrated perspective on carbon storage across the main sedimentary environments in the study area.

4.8. Radiocarbon Ages and Age-Depth Models

Twenty-four AMS radiocarbon dates of estuarine shell material were obtained from four sediment cores: Cores B, D, E, and H (Table S3 in Supporting Information S1). Calibrated ages ranged from 190 ± 180 cal yrs BP (Core B; 0.45 m depth) to 7,100 ± 180 cal yrs BP (Core D; 2.80 m depth). Two samples from Core E, dated to 1964 and 1965 AD based on post-bomb radiocarbon signatures (104.1 ± 0.3% and 106.0 ± 0.3% pMC), represent modern sediment accumulation and were retained in age-depth modeling to constrain recent depositional history.

Core D captures the longest stratigraphic record, extending from ∼7,700 cal yrs BP to the present (Figure 11a). Core E spans from ∼1,600 cal yrs BP to the present (Figure 11b). Core H preserves a succession from ∼3,400 cal yrs BP to the present (Figure 11c).

Age-depth models for Cores D and E indicate hiatuses in their stratigraphy, in contrast to relatively continuous sedimentation in Core H. In Core D, a depositional break separates sediments older than ∼5,700 cal yrs BP from sediments younger than ∼3,400 cal yrs BP (Figure 11a). In Core E, the break separates sediments older than ∼350 cal yrs BP from sediments younger than ∼70 cal yrs BP (Figure 11b). These depositional hiatuses represent a gap in time of ∼2,300 and ∼280 cal yrs BP, respectively.

5. Discussion

5.1. Spatial-Temporal Patterns of Organic Carbon Burial by Facies

To better understand the spatial and temporal patterns of OC accumulation across Ōhiwa Harbor, and in relation to sedimentary facies, the facies specific sediment accumulation rates and OC storage rates over the past ∼7,700, ∼1,600, ∼3,400 cal yrs BP in the three age-modeled cores were compared. Variations in facies distribution and accumulation rates reveal how depositional (sub) environments, and thus sedimentary facies, have influenced OC burial (Figure 12; Table 2).

Along the sheltered southwestern margin of Ōhiwa Harbor, Core D preserves ∼7,700 yrs of alternating upper tidal-flat muds (Facies F5), shell-bed layers (Facies F1), and bioturbated sandy facies (Facies F3) (Figure 12a). At the base of the cored succession (∼7,700–5,691 yrs BP; 310–192 cm depth), deposition was dominated by frequent facies alternations with moderate sediment accretion rates ranging from 0.45 to 1.11 mm yr^{-1}. Organic carbon burial during this interval was steady but moderate, from 2.60 to 8.70 × 10^{-4} g cm^{-2} yr^{-1}, with the highest organic carbon storage rates associated with intervals of Facies F3 and F5. A pronounced hiatus occurred between ∼5,691 and 3,336 yrs BP (∼192 cm depth), after which deposition resumed with lower tidal-flat sands and more consistent sediment accumulation (0.46–0.73 mm yr^{-1}). Strata deposited after the depositional hiatus show sustained organic carbon burial (1.60–6.70 × 10^{-4} g cm^{-2} yr^{-1}). The stratigraphy of Core D shows a transition from dynamic, frequently reworked substrates in the early Holocene to steadier sedimentation and organic carbon retention in the late Holocene.

Near the south-central portion of Ōhiwa Harbor, Core E is located closer to the main tidal channel bifurcation, recording ∼1,600 yrs of deposition. Sedimentary facies are dominated by lower tidal-flat sands and muddy sands (Facies F3), with intermittent shell-bed layers (Facies F1) and brief muddy intervals of bioturbated muds (Facies F5) (Figure 12b). Early in the depositional record (∼1,553–950 yrs BP; 210–114 cm depth), Facies F3 was dominant, with relatively high sediment accretion rates (1.16–1.85 mm yr^{-1}) and organic carbon burial rates of 3.40 × 10^{-4}–1.86 × 10^{-3} g cm^{-2} yr^{-1}. A pulse of deposition of Facies F5 (114–101 cm; 950–880 yrs BP) corresponds to the highest organic carbon storage rate observed in Core E (3.71 × 10^{-3} g cm^{-2} yr^{-1}). After about 880 yrs BP (101–0 cm depth), deposition alternated between Facies F3 and Facies F1, with sediment accretion remaining relatively high (1.32–1.57 mm yr^{-1}) and organic carbon burial steady (4.30 × 10^{-4}–

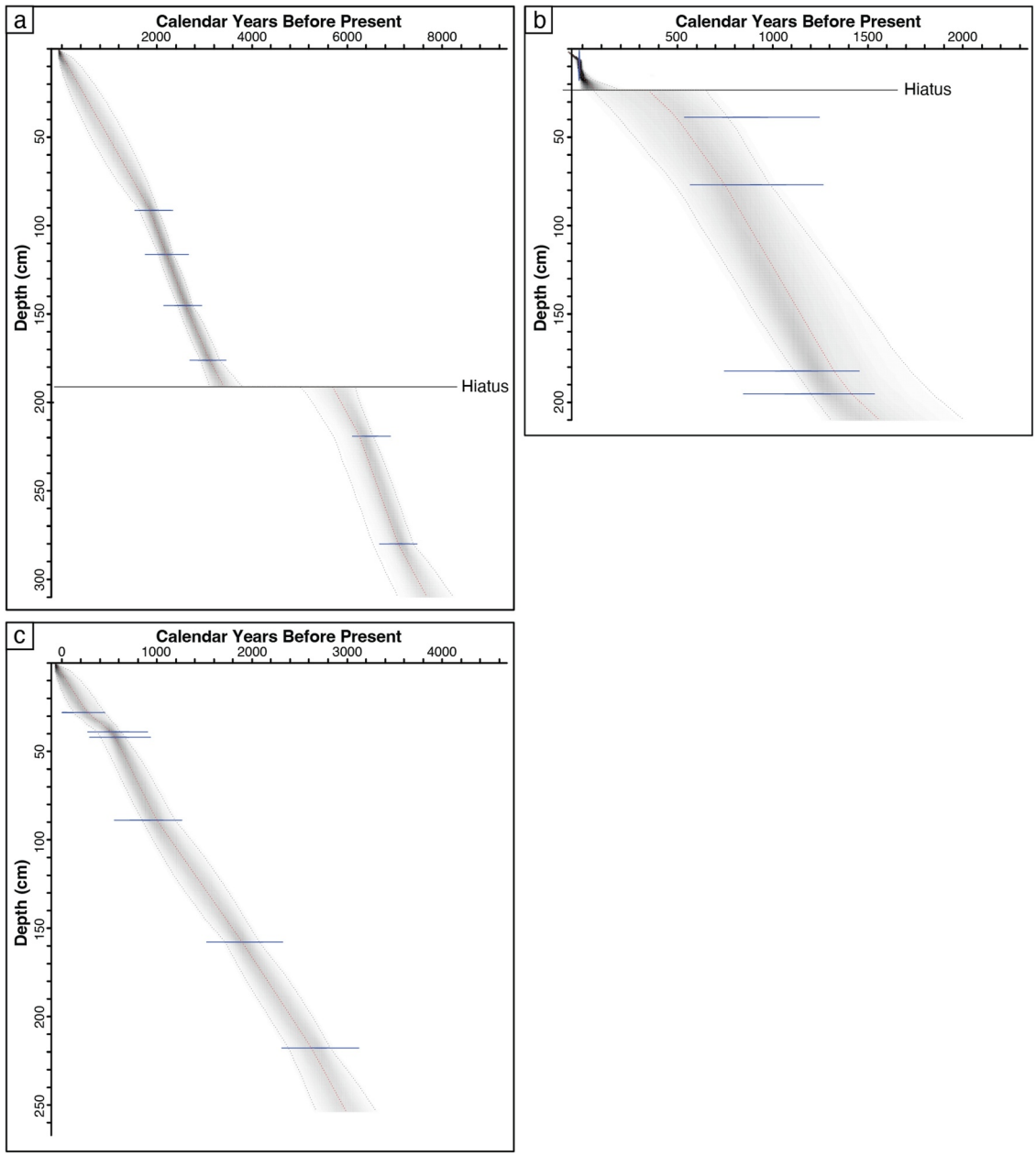

Figure 11. Bayesian age-depth models, constrained by radiocarbon dating of estuarine shells, for: (a) Core D, (b) Core E, and (c) Core H. Depositional hiatuses are present in Cores D and E, which are supported by sedimentologic and stratigraphic evidence. Modeling was undertaken in rBacon (Blaauw & Christen, 2011).

2.38×10^{-3} g cm^{-2} yr^{-1}). The stratigraphy of Core E demonstrates an active depositional setting with relatively rapid sedimentation and frequent facies shifts. These conditions were suitable to maintain high organic carbon storage through the late Holocene.

Situated nearer the harbor mouth, Core H records ~3,400 yrs of deposition characterized by alternating upper tidal-flat muds (Facies F5) and shell-bed deposits (Facies F1), with occasional lower tidal-flat sands (Facies F3) (Figure 12c). The oldest part of the record (3,413–2,142 yrs BP; 254–197 cm depth), was characterized by alternating beds of Facies F1 and F5 demonstrating moderate sediment accretion rates (0.44–0.88 mm yr^{-1}) and organic carbon burial of 3.60–5.70 $\times$ 10^{-4} g cm^{-2} yr^{-1}. The younger strata (2,142 yrs BP–present; 197–0 cm depth), display similar sediment accumulation rates (0.62–0.87 mm yr^{-1}) and fairly stable organic carbon storage

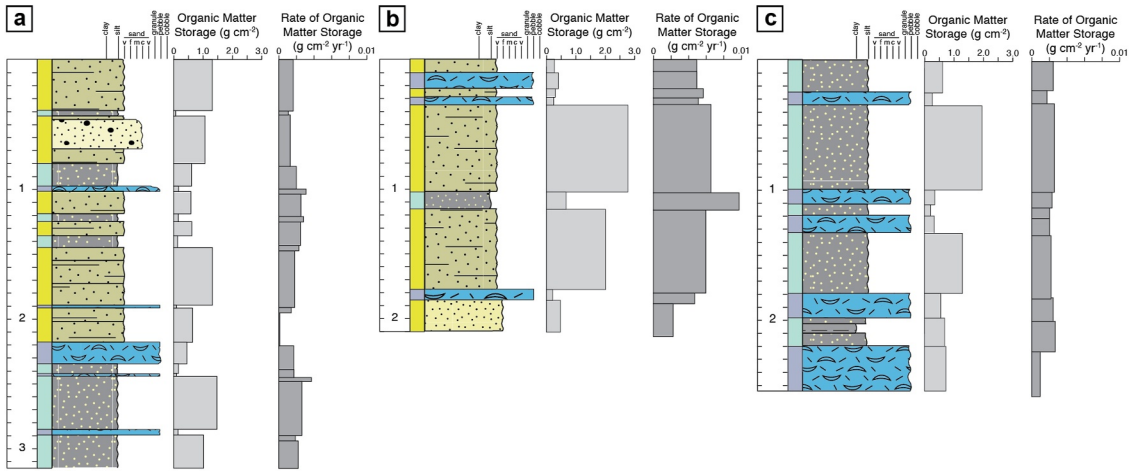

Figure 12. Stratigraphy, organic carbon storage (g cm^{-2}), and rate of organic carbon storage (g cm^{-2} yr^{-1}) for: (a) Core D, (b) Core E, and (c) Core H. These are measured over the last ~7,700, ~1,600, and ~3,400 yrs ago, respectively.

(2.50–5.40 × 10^{-4} g cm^{-2} yr^{-1}). Core H was characterized by persistent moderate-energy deposition with repeated switching of facies, acting to control sediment texture and organic carbon retention.

When all three cores are compared it becomes clear that depositional setting and facies type strongly influenced organic carbon accumulation. In sheltered areas (Core D), sediment accumulation and organic carbon burial rates are moderate. Higher sediment accumulation and organic carbon storage rates are characteristic of Core E, located closer to the main tidal channel. Finally, near the harbor mouth in Core H, sediment accumulation rates are moderate with stable but lower organic carbon burial than in Core E. These results suggest that energy conditions and sediment type, through their control on facies, jointly determine the propensity for organic carbon burial over long timescales.

5.2. Depositional Facies Controls on Organic Carbon Burial

The sedimentological and stratigraphic data from cores and surface sediments in Ōhiwa Harbor demonstrate that OM/OC burial closely relates to sedimentary facies. The facies classification captures differences in sedimentary texture, physical structure, and biogenic characteristics of the sediment, which reflect local physico-chemical environmental conditions. Mud-dominated facies, such as Facies F4, are characterized by the highest OC concentrations. The laminated nature of Facies F4, which generally lacks bioturbation, suggests limited oxygen penetration into the sediment and/or rapid sedimentation rates, providing ideal conditions for OC preservation (Burdige, 2007; Hedges & Keil, 1995). This differs somewhat from Facies F3 and F5, which display moderate bioturbation intensity but still contain relatively high OC content, and indication of sediment accumulation rates outpacing the decomposition of OM. Coarse grained facies like Facies F2, by contrast, are deposited in high energy areas such as tidal creeks and channels. These regions have low OC density due to frequent sediment reworking and poor cohesive sediment retention which limits sequestration.

Hydrodynamic modeling undertaken by Bryan et al. (2023) supports the facies based observations of this study. Their simulations showed that the upper tidal flats and sheltered bay areas of Ōhiwa Harbor were the main zones of fine sediment accumulation due to low current velocities and longer water-sediment residence times. These are the areas where this study has shown Facies F4 and F5, and to a lesser extent Facies F3, accumulate. Meanwhile, the higher energy zones near the harbor entrance are where coarse grained and OC-poor deposits accumulate, typical of Facies F2. The dominance of OC-rich facies in the harbor over the last ~7,700 yrs (Figure 12) suggests a long period of stable depositional conditions that favored carbon burial, despite fluctuations in sea level, sediment supply, and harbor morphology. However, recent increases in sediment accumulation, estimated to be 3–6 times natural levels because of land-use changes, raise concerns that human activity could upset benthic processes or overwhelm carbon storing environments (Bryan et al., 2023).

Facies deposited under moderate or fluctuating energy levels, like Facies F5, appear to strike a balance between sediment burial and reworking, potentially maximizing carbon storage. Shifts in facies distribution patterns with

Table 2
Sediment Accretion Rates and Organic Carbon Storage Metrics by Facies and Depth Interval for Cores D, E, and H

Core	Facies	From (cm)	To (cm)	From age (yrs BP)	To age (yrs BP)	Sediment accretion rate (mm yr^{-1})	OC stored (g cm^{-2})	OC storage rate (g cm^{-2} yr^{-1})
D	F5	310	289	7,668	7,204	0.453	0.284	6.60×10^{-4}
D	F1	289	285	7,204	7,124	0.500	0.037	4.60×10^{-4}
D	F5	285	244	7,124	6,560	0.727	0.362	7.80×10^{-4}
D	F1	244	241	6,560	6,533	1.111	0.024	7.80×10^{-4}
D	F5	241	235	6,533	6,440	0.645	0.034	5.30×10^{-4}
D	F1	235	217	6,440	6,173	0.674	0.086	4.10×10^{-4}
D	F3	217	192	6,173	5,691	0.519	0.123	2.60×10^{-4}
D	F1	192	188	3,407	3,336	0.563	0.019	3.10×10^{-4}
D	F3	188	145	3,336	2,596	0.581	0.294	4.00×10^{-4}
D	F5	145	141	2,596	2,539	0.702	0.030	6.30×10^{-4}
D	F3	141	123	2,539	2,286	0.711	0.149	6.90×10^{-4}
D	F5	123	119	2,286	2,229	0.702	0.04	8.70×10^{-4}
D	F3	119	102	2,229	1,995	0.726	0.143	6.70×10^{-4}
D	F1	102	98	1,995	1,940	0.727	0.043	8.50×10^{-4}
D	F5	98	81	1,940	1,633	0.554	0.153	4.60×10^{-4}
D	F3	81	42	1,633	808	0.473	0.210	2.30×10^{-4}
D	F5	42	39	808	743	0.462	0.012	1.60×10^{-4}
D	F3	39	0	743	−64	0.483	0.308	3.00×10^{-4}
E	F3	210	185	1,553	1,338	1.163	0.066	3.40×10^{-4}
E	F1	185	177	1,338	1,291	1.702	0.045	1.26×10^{-3}
E	F3	177	114	1,291	950	1.848	0.466	1.86×10^{-3}
E	F5	114	101	950	880	1.857	0.193	3.71×10^{-3}
E	F3	101	34	880	451	1.562	0.736	2.38×10^{-3}
E	F1	34	29	451	402	1.020	0.065	1.03×10^{-3}
E	F3	29	22	402	349	1.321	0.076	1.29×10^{-3}
E	F1	22	9	71	−12	1.566	0.095	8.00×10^{-4}
E	F3	9	0	−12	−69	1.579	0.056	4.30×10^{-4}
H	F1	254	220	3,413	2,636	0.438	0.116	3.60×10^{-4}
H	F5	220	197	2,636	2,373	0.875	0.157	5.70×10^{-4}
H	F1	197	179	2373	2,142	0.779	0.119	4.80×10^{-4}
H	F5	180	132	2142	1,548	0.808	0.267	4.10×10^{-4}
H	F1	132	119	1,548	1,380	0.774	0.067	3.50×10^{-4}
H	F5	119	111	1,380	1,276	0.769	0.043	3.70×10^{-4}
H	F1	111	99	1,276	1,120	0.769	0.076	4.50×10^{-4}
H	F5	99	32	1,120	346	0.866	0.426	5.40×10^{-4}
H	F1	32	22	346	185	0.621	0.058	2.50×10^{-4}
H	F5	22	0	185	−69	0.866	0.132	3.20×10^{-4}

Note. Age estimates are based on radiocarbon-derived Bayesian age models. OC stored represents cumulative OC per unit area, and OC storage rate represents time-normalized OC burial. Negative ages represent yrs after 1950 (0 BP in radiocarbon dating).

time and amongst cores show clearly that OC burial potential varies with channel migration, sediment supply, and local morphology. While levels of OM and OC differ among facies, bioturbation and physical mixing of sediment continually redistribute organic matter. Thus sedimentary (sub) environments and their sedimentary facies are dynamic systems rather than fixed carbon reservoirs.

5.3. Comparison of Carbon Stocks Across Aotearoa and Beyond

Stocks of organic carbon in the upper meter of sediment in Ōhiwa Harbor range from 56 to 120 t C ha^{-1}, with the highest stocks occurring in the most sheltered, fine-grained locations. These values are comparable to, or higher than, OC stocks reported from vegetated habits elsewhere in Aotearoa New Zealand. In Tairua Estuary, for example, Bulmer et al. (2020) reported carbon stocks of 85 t C ha^{-1} for saltmarsh, 46 t C ha^{-1} for mangroves, and 27 t C ha^{-1} for seagrass, while unvegetated tidal flats contained only 26 t C ha^{-1}. Larger scale national syntheses indicate that OC stocks (to 100 cm depth) in mangroves and saltmarsh typically range from 38 to 85 t C ha^{-1} (Bulmer et al., 2020; Ho et al., 2023; Ross et al., 2024). At Onetāhua/Farewell Spit, Berthelsen et al. (2023) found that seagrass meadows generally store less carbon, with stocks around 17 t C ha^{-1} (to 40 cm depth). Perhaps the most significant aspect of our finding that Ōhiwa Harbor's unvegetated tidal flats have relatively large OC stocks is that they occupy a much greater area than the vegetated part of the system. Chen et al. (2020) emphasized this aspect in their study of Chinese tidal flats, noting that unvegetated tidal flats account for ~80% of C (78 Tg C to 100 cm).

In the global context, Ōhiwa Harbor's unvegetated tidal flat OC stocks fall within the middle to upper range. Synthesizing data from 190 locations worldwide, Chen and Lee (2022) showed that unvegetated tidal flats sequester on average 86 t C ha^{-1} OC (to 100 cm depth). Mazarrasa et al. (2023)'s compilation of unvegetated coastal systems in Europe estimated carbon stocks to average about 46 t C ha^{-1}, slightly lower than high marsh (65 t C ha^{-1}) but greater than low marsh (38 t C ha^{-1}) and seagrass (40 t C ha^{-1}). Together these results demonstrate that unvegetated soft sediments can store carbon at magnitudes comparable to vegetated substrates when depositional conditions favor accumulation and preservation.

5.4. Potential Influence of Seagrass and Mangroves

Ōhiwa Harbor is the southern extent of mangroves on the east coast of Aotearoa New Zealand's North Island, and thus, it is important to consider the contribution of mangroves, as well as saltmarsh and seagrass to OC stocks in the unvegitated tidal flat sediments. Cores collected near mangrove or seagrass (i.e., cores B, E, and G) were observed to only show modest OC enrichment (Figure 13). Rather, the maximum OC values occur in muddy, low-energy facies, which are not directly adjacent to vegetation. Nevertheless, vegetation likely contributes locally to OC concentrations through organic matter export and trapping of fine-grained sediment (Bulmer et al., 2020). Collectively, these results show that sedimentary environment, rather than vegetation cover, governs the magnitude and spatial pattern of organic carbon storage in Ōhiwa Harbor.

5.5. Implications for Blue Carbon Accounting and Budgets

The results presented in this study show the importance of moving beyond bulk sediment characterization for blue carbon accounting, given that sedimentary facies and depositional (sub) environment are so important to OM/OC accumulation. Explicitly linking physical processes to long-term storage provides a means to better predict carbon burial efficiency in unvegetated coastal sediments, which depend as much on the nature and stability of deposition than on the presence of nearby vegetation. These details are often masked within large-scale studies, but differences within "unvegetated" categories are important for blue-carbon accounting frameworks. Such process-based approaches have been urged in recent studies (Chen & Lee, 2022; Mazarrasa et al., 2023).

The facies resolved data set from this study provides stratigraphically constrained sediment accumulation rates and OC stocks, which can be used in future regional or national scale coastal carbon budgets. The detailed information about sedimentary facies and age control are useful for scaling of carbon burial to sedimentary environment, contributing to reducing uncertainties in carbon inventories that usually rely on generic coefficients (Chen & Lee, 2022; Zhou et al., 2024).

Sedimentary environment, rather than vegetation alone, plays a first order control on coastal carbon stores and their resilience. Future work should continue to focus on recognizing depositional settings that favor long-term retention, which are generally characterized by fine grained, minimally disturbed facies. These will broaden the scope of blue carbon management efforts to include unvegetated tidal flats and their connections to vegetated habits. Maintaining sediment supply and limiting physical disturbance may therefore yield mitigation benefits comparable to habitat restoration. Preserving stable, fine-grained intertidal flats is as critical to coastal-carbon resilience as conserving mangroves or saltmarshes (Chen & Lee, 2022; Ho et al., 2023).

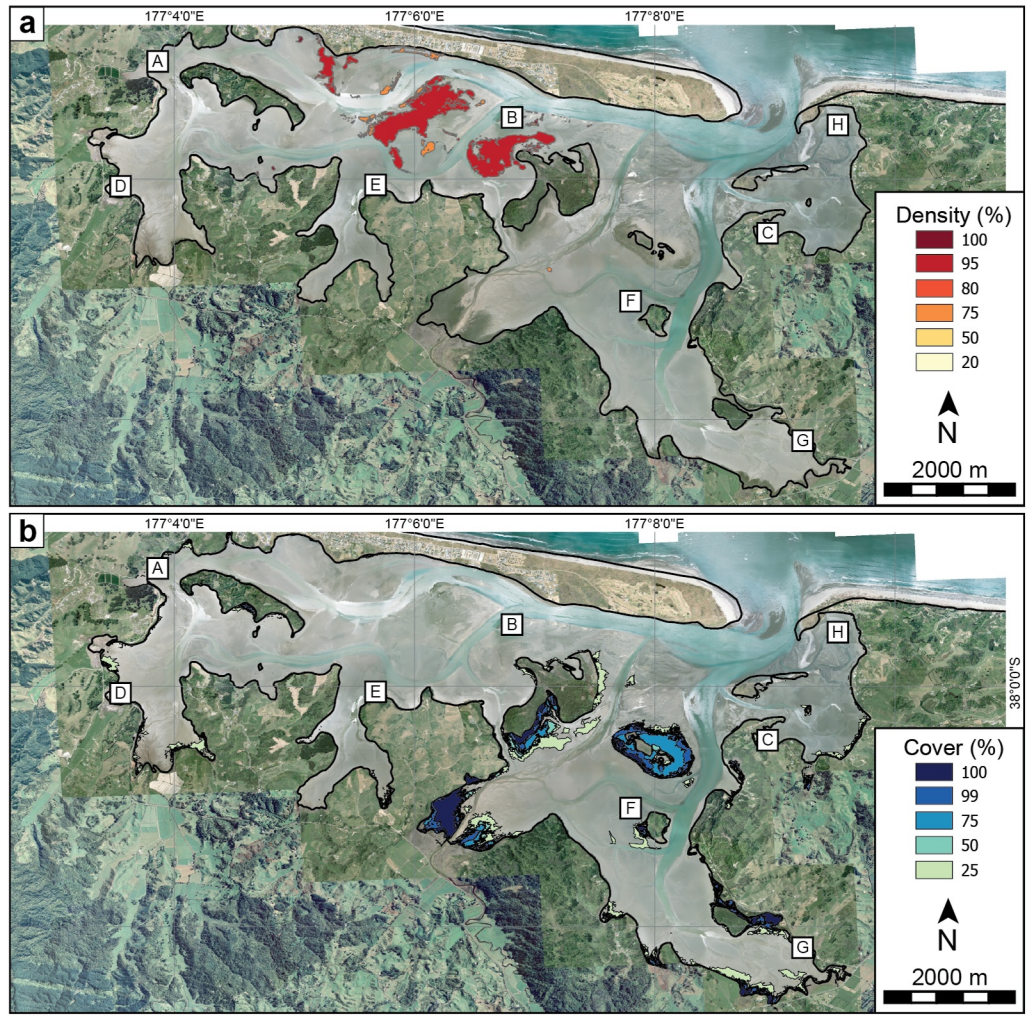

Figure 13. (a) Distribution and density of seagrass habitat in Ōhiwa Harbor from 2011. (b) Distribution and cover of mangrove habitat from 2011. Data from Bay of Plenty Regional Council Environment Map Server (https://gis.boprc.govt.nz/server2/rest/services/BayOfPlentyMaps/Environment/MapServer), used under the Creative Commons Attribution 4.0 International license. Modifications were made to symbology.

6. Conclusions

Analysis of three radiocarbon-dated sediment cores and surface sediments from Ōhiwa Harbor demonstrates that sedimentary facies control OM/OC accumulation and burial in unvegetated intertidal flats. Five distinct depositional facies are observed in the estuary, each with characteristic carbon density and burial rates. Mud-rich, low-energy facies such as rippled mud and bioturbated mud consistently support the highest OC burial, while sandy, higher-energy facies store substantially less OC.

Both spatial and temporal variations in carbon sequestration reflect changes in depositional environment over the past ~7,700 yrs. As depositional environments migrated and energy regimes fluctuated, the balance between storage and loss also changed. These results show that carbon sequestration in unvegetated tidal flats is neither static nor spatially uniform but evolves with the persistence and distribution of fine-grained facies.

Although vegetated habitats border parts of Ōhiwa Harbor, their direct influence on carbon stocks within unvegitated tidal flats appears limited. Instead, organic-matter preservation depends primarily on physical sedimentary conditions and the stability of low-energy depositional zones. Carbon storage in these sediments is therefore primarily a sedimentological phenomenon.

Recognizing facies as the key organizing unit provides a practical framework for extending blue-carbon accounting beyond vegetated habitats. Protecting and maintaining fine-grained, low-energy tidal flats through careful management of sediment supply and hydrodynamic disturbance may be as critical for coastal-carbon resilience as conserving mangroves or saltmarsh.

Conflict of Interest

The author declares no conflicts of interest relevant to this study.

Data Availability Statement

Sedimentologic, organic matter, and organic carbon data used in this study can be accessed at La Croix (2025).

Acknowledgments
Thanks to Ben Roche, Ben Stewart, and Chris Morcom for assistance in the field. Daniel Bruce is acknowledged for his work on carbon-dating shells. Holly Harvey-Wishart assisted with LOI analysis. Discussions and field trips to the harbor with Karin Bryan and Kura Paul-Burke gave important context to the study. Ngāti Awa, the mana whenua, are thanked for their engagement and support of this research. Stephen Park and the Bay of Plenty Regional Council provided funding, as did ASLO's Global Outreach Initiative. Carbon analysis was undertaken at NIWA's Environmental and Ecological Stable Isotope Facility. Thoughtful reviews by Massimiliano Ghinassi and an anonymous reviewer improved the clarity of the paper.

References

Alongi, D. M. (2020). Carbon balance in salt marsh and mangrove ecosystems: A global synthesis. *Journal of Marine Science and Engineering*, *8*(10), 767. https://doi.org/10.3390/jmse8100767

Baas, J. H., & Best, J. L. (2008). The dynamics of turbulent, transitional and laminar clay-laden flow over a fixed current ripple. *Sedimentology*, *55*(3), 635–666. https://doi.org/10.1111/j.1365-3091.2007.00916.x

Bauer, J. E., Cai, W.-J., Raymond, P. A., Bianchi, T. S., Hopkinson, C. S., & Regnier, P. A. G. (2013). The changing carbon cycle of the coastal ocean. *Nature*, *504*(7478), 61–70. https://doi.org/10.1038/nature12857

Beanland, S., & Berryman, K. R. (1992). Holocene coastal evolution in a continental rift setting: Bay of Plenty, New Zealand. *Quaternary International*, *15/16*, 151–158. https://doi.org/10.1016/1040-6182(92)90043-2

Berthelsen, A., Walker, A., Skilton, J., Chamberose, S., Flewitt, S., Waters, S., et al. (2023). *Sediment organic carbon stocks in coastal blue carbon habitats: Pilot study for Te Tauihu, Report No. 3867* (p. 31). Cawthron Institute.

Bianchi, T. S., Cui, X., Blair, N. E., Burdige, D. J., Eglinton, T. I., & Galy, V. (2018). Centers of organic carbon burial and oxidation at the land-ocean interface. *Organic Geochemistry*, *115*, 138–155. https://doi.org/10.1016/j.orggeochem.2017.09.008

Blaauw, M., & Christen, J. A. (2011). Flexible paleoclimate age-depth models using an autoregressive gamma process. *Bayesian Analysis*, *6*(3), 457–474. https://doi.org/10.1214/ba/1339616472

Blott, S. J., & Pye, K. (2001). GRADISTAT: A grain size distribution and statistics package for the analysis of unconsolidated sediments. *Earth Surface Processes and Landforms*, *26*(11), 1237–1248. https://doi.org/10.1002/esp.261

Bronk Ramsey, C. (1995). Radiocarbon calibration and analysis of stratigraphy: The OxCal program. *Radiocarbon*, *37*(2), 425–430. https://doi.org/10.1017/S0033822200030903

Bryan, K. R., Stewart, B., Rahdarian, A., & Rautenbach, C. (2023). *Ōhiwa Harbour Delft3D sediment transport modelling to support the National Policy Statement on Freshwater (NPS-FM),* Environmental Research Insititute Report No. 162, Environmental Research Institute, Division of Health, Engineering, Computing & Science, (p. 67).

Bulmer, R. H., Stephenson, F., Jones, H. F. E., Townsend, M., Hillman, J. R., Schwendenmann, L., & Lundquist, C. J. (2020). Blue carbon stocks and cross-habitat subsidies. *Frontiers in Marine Science*, *7*(380), 380. https://doi.org/10.3389/fmars.2020.00380

Burdige, D. J. (2007). Preservation of organic matter in marine sediments: Controls, mechanisms, and an imbalance in sediment organic carbon budgets? *Chemical Reviews*, *107*(2), 467–485. https://doi.org/10.1021/cr050347q

Chen, J., Wang, D., Li, Y., Yu, Z., Chen, S., Hou, X., et al. (2020). The carbon stock and sequestration rate in tidal flats from coastal China. *Global Biogeochemical Cycles*, *34*(11), e2020GB006772. https://doi.org/10.1029/2020GB006772

Chen, Z. L., & Lee, S. Y. (2022). Tidal flats as a significant carbon reservoir in global coastal ecosystems. *Frontiers in Marine Science*, *9*, 900896. https://doi.org/10.3389/fmars.2022.900896

Dalrymple, R. W., Zaitlin, B. A., & Boyd, R. (1992). Estuarine facies models; conceptual basis and stratigraphic implications. *Journal of Sedimentary Research*, *62*(6), 1130–1146. https://doi.org/10.1306/d4267a69-2b26-11d7-8648000102c1865d

Freestone, H. J. (1976). *Report of a full cycle tidal Gaugin carried out at the Ohiwa Harbor entrance, 6 April 1976, Unpublished report*. Ministry of Works and Development, Rotorura.

Gibb, J. G. (1977). *Late Quaternary sedimentary processes at Ohiwa Harbour, eastern Bay of Plenty with special reference to property loss on Ohiwa Spit, Water and Soil Technical Publication No. 5* (p. 16). Ministry of Works and Development.

Hayward, B. W., Cochran, U., Southall, K., Wiggins, E., Grenfell, H. R., Sabaa, A., et al. (2004). Micropalaeontological evidence for the Holocene earthquake history of the eastern Bay of Plenty, New Zealand, and a new index for determining the land elevation record. *Quaternary Science Reviews*, *23*(14–15), 1651–1667. https://doi.org/10.1016/j.quascirev.2004.01.010

Healy, J. (1967). Geology of Whakatane. *Whakatane Historical Review*, *15*, 9–26.

Healy, T. R. (1978). *Some textural and mineralogical investigations of the Rangitaiki Plains foreshore and river sands, Bay of Plenty Coastal Survey Report, Bay of Plenty Catchment Commission* (p. 74). Whakatane.

Heaton, T. J., Köhler, P., Butzin, M., Bard, E., Reimer, R. W., Austin, W. E. N., et al. (2020). Marine20—The marine radiocarbon age calibration curve (0–55,000 cal BP). *Radiocarbon*, *62*(4), 779–820. https://doi.org/10.1017/RDC.2020.68

Hedges, J. I., & Keil, R. G. (1995). Sedimentary organic matter preservation: An assessment and speculative synthesis. *Marine Chemistry*, *49*(2–3), 81–115. https://doi.org/10.1016/0304-4203(95)00008-f

Ho, M., Berthelsen, A., & Clark, D. (2023). *Blue carbon habitats in the Otago region, Report No. 3963* (p. 33). Cawthron Institute, Nelson.

Julian, K. A. (2006). *Coastal processes influencing beach erosion at Ohope Spit* (Master's thesis). University of Waikato.

La Croix, A. D. (2025). Sedimentologic, organic matter, and organic carbon data from Ōhiwa Harbor, Aotearoa New Zealand [Dataset]. *Zenodo*. https://doi.org/10.5281/zenodo.17644699

La Croix, A. D., & Gingras, M. K. (2021). Facies characteristics and stratigraphy of an Upper Cretaceous mud-dominated subaqueous delta: Medicine Hat member (Niobrara formation), Alberta, Canada. *Sedimentology*, *68*(6), 2820–2853. https://doi.org/10.1111/sed.12875

La Croix, A. D., Roche, B., & Mullarney, J. C. (2025). Dynamic mud deposition along the fluvial-tidal transition zone in the Waihou river, Aotearoa New Zealand. *Journal of Geophysical Research: Earth Surface*, *130*(130), e2024JF007817. https://doi.org/10.1029/2024JF007817

Lambeck, K., Rouby, H., Purcell, A., Sun, Y., & Sambridge, M. (2014). Sea level and global ice volumes from the last glacial maximum to the Holocene. *Proceedings of the National Academy of Sciences of the USA*, *111*(43), 15296–15303. https://doi.org/10.1073/pnas.1411762111

Lee, J., Kim, B., Noh, J., Lee, C., Kwon, I., Kwon, B.-O., et al. (2021). The first national scale evaluation of organic carbon stocks and sequestration rates of coastal sediments along the West sea, south sea, and east sea of South Korea. *Science of the Total Environment*, *793*, 148568. https://doi.org/10.1016/j.scitotenv.2021.148568

MacKay, D. A., & Dalrymple, R. W. (2011). Dynamic mud deposition in A tidal environment: The record of fluid-mud deposition in the Cretaceous Bluesky formation, Alberta, Canada. *Journal of Sedimentary Research*, *81*(12), 901–920. https://doi.org/10.2110/jsr.2011.74

Manning, D. A. (1996). Middle-late Pleistocene tephrostratigraphy of the eastern Bay of Plenty, New Zealand. *Quaternary International*, *34–36*, 3–12. https://doi.org/10.1016/1040-6182(95)00064-x

Mayer, L. M. (1994). Surface area control of organic carbon accumulation in continental shelf sediments. *Geochimica et Cosmochimica Acta*, *58*(4), 1271–1284. https://doi.org/10.1016/0016-7037(94)90381-6

Mayer, L. M., Rahaim, P. T., Guerin, W., Macko, S. A., Watling, L., & Anderson, F. E. (1985). Biological and granulometric controls on sedimentary organic matter of an intertidal mudflat. *Estuarine, Coastal and Shelf Science*, *20*(4), 491–503. https://doi.org/10.1016/0272-7714(85)90091-5

Mazarrasa, I., Neto, J. M., Bouma, T. J., Grandjean, T., Garcia-Orellana, J., Masqué, P., et al. (2023). Drivers of variability in blue Carbon stocks and burial rates across European estuarine habitats. *Science of the Total Environment*, *886*, 163957. https://doi.org/10.1016/j.scitotenv.2023.163957

Mcleod, E., Chmura, G. L., Bouillon, S., Salm, R., Björk, M., Duarte, C. M., et al. (2011). A blueprint for blue carbon: Toward an improved understanding of the role of vegetated coastal habitats in sequestering CO_2. *Frontiers in Ecology and the Environment*, *9*(10), 552–560. https://doi.org/10.1890/110004

Murdoch, B. G. (2005). *Holocene evolution of ohope barrier spit, eastern Bay of Plenty, North Island, New Zealand* (Master's thesis). University of Waikato.

Puppin, A., Tognin, D., Ghinassi, M., Franceschinis, E., Realdon, N., Marani, M., & D'Alpaos, A. (2024). Spatial patterns of organic matter content in the surface soil of the salt marshes of the Venice lagoon (Italy). *Biogeosciences*, *21*(12), 2937–2954. https://doi.org/10.5194/bg-21-2937-2024

Richmond, B. M., Nelson, C. S., & Healy, T. R. (1984). Sedimentology and evolution of Ohiwa Harbor, a barrier-impounded estuarine lagoon in Bay of Plenty. *New Zealand Journal of Marine & Freshwater Research*, *18*(4), 461–478. https://doi.org/10.1080/00288330.1984.9516068

Ross, F. W. R., Clark, D. E., Albot, O., Berthelsen, A., Bulmer, R., Crawshaw, J., & Macreadie, P. I. (2024). A preliminary estimate of the contribution of coastal blue carbon to climate change mitigation in New Zealand. *New Zealand Journal of Marine & Freshwater Research*, *58*(3), 530–540. https://doi.org/10.1080/00288330.2023.2245770

Serrano, O., Lavery, P. S., Duarte, C. M., Kendrick, G. A., Calafat, A., York, P. H., et al. (2016). Can mud (silt and clay) concentration be used to predict soil organic carbon content within seagrass ecosystems? *Biogeosciences*, *13*(17), 4915–4926. https://doi.org/10.5194/bg-13-4915-2016

Taylor, A. M., & Goldring, R. (1993). Description and analysis of bioturbation and ichnofabric. *Journal of the Geological Society of London*, *150*(1), 141–148. https://doi.org/10.1144/gsjgs.150.1.0141

Wood, J. C. (2015). Determination of moisture content and total organic carbon within basin environments: Loss-on-ignition. In L. E. Clarke & J. M. Nield (Eds.), *Geomorphological techniques (online edition)* (pp. 1–7). British Society for Geomorphology.

Zhou, J., Zhang, L., Zhang, J., Gan, S., Lu, Z., Qin, G., et al. (2024). Blue carbon storage of tidal flats and salt marshes: A comparative assessment in two Chinese coastal areas. *Palaeogeography, Palaeoclimatology, Palaeoecology*, *655*, 112509. https://doi.org/10.1016/j.palaeo.2024.112509